SIRT3 deSUMOylation sustains hematopoietic stem cell activities under stressful conditions via the DHX58-IRF7 axis

Xiaoxiao He,[1,2*] Jing Yu,[2*] Yilu Xu,[2*] Tianshi Wang,[3,4] Yang Lu,[2] Jiaxin Wu,[2] Sijia Dan,[2] Yiqiu Xia,[2] Xingmei Mu,[2] Li Xie,[2] Chiqi Chen,[2] Zhuo Yu,[2] Jing Ye,[5-7] Eric Gilson,[5,8,9] Yaping Zhang,[2] Jinke Cheng[3,10,11] and Junke Zheng[2,12]

[1]Department of Hematology, Xinhua Hospital, Shanghai Jiao Tong University School of Medicine, Shanghai, China; [2]Institute for Translational Medicine on Cell Fate and Disease, Shanghai Ninth People's Hospital, Key Laboratory of Cell Differentiation and Apoptosis of National Ministry of Education, Department of Pathophysiology, Shanghai Jiao Tong University School of Medicine, Shanghai, China; [3]Shanghai Key Laboratory for Tumor Microenvironment and Inflammation, Department of Biochemistry and Molecular Cell Biology, Shanghai Jiao Tong University School of Medicine, Shanghai, China; [4]Department of Nephrology, Renji Hospital, Shanghai Jiao Tong University School of Medicine, Shanghai, China; [5]International Laboratory in Hematology, Cancer, Aging and Hematology, Pôle Sino-Français de Recherche en Sciences du Vivant et Génomique, Ruijin Hospital, Shanghai Jiao Tong University School of Medicine/CNRS/INSERM/University Côte d'Azur, Shanghai, China; [6]The State Key Laboratory of Medical Genomics, Shanghai, China; [7]Department of Geriatrics, Medical Center on Aging of Shanghai Ruijin Hospital, Shanghai Jiaotong University School of Medicine, Shanghai, China; [8]University Côte d'Azur, Inserm, CNRS, IRCAN, Nice, France; [9]Department of Medical Genetics, IHU RespirERA, CHU, Nice, France; [10]Institute of Aging & Tissue Regeneration, RenJi Hospital, Shanghai Jiao Tong University School of Medicine, Shanghai, China; [11]Hainan Academy of Medical Sciences, Haikou Hainan, China and [12]Shanghai Key Laboratory of Reproductive Medicine, Shanghai Jiao Tong University School of Medicine, Shanghai, China

**XH, JYu and YXu contributed equally as first authors.*

Correspondence: J. Zheng
zhengjunke@shsmu.edu.cn

J. Cheng
jkcheng@shsmu.edu.cn

Y. Zhang
yapingzhang1117@126.com

E. Gilson
Eric.Gilson@unice.fr

X. He
xiaoxiaohe@sjtu.edu.cn

Received: October 15, 2025.
Accepted: April 24, 2026.
Early view: April 30, 2026.

https://doi.org/10.3324/haematol.2025.300025

©2026 Ferrata Storti Foundation
Published under a CC BY-NC license

Figure S1

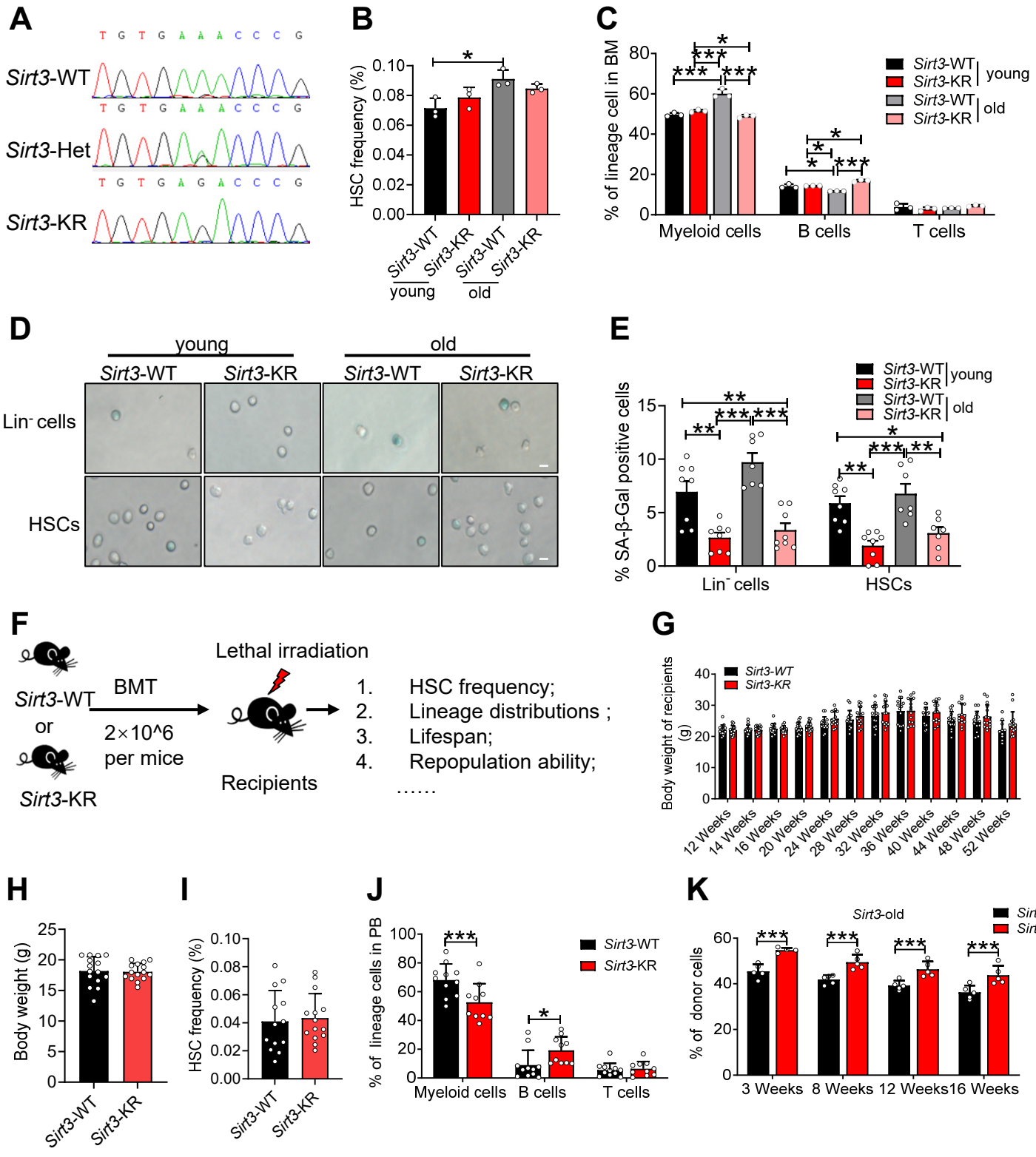
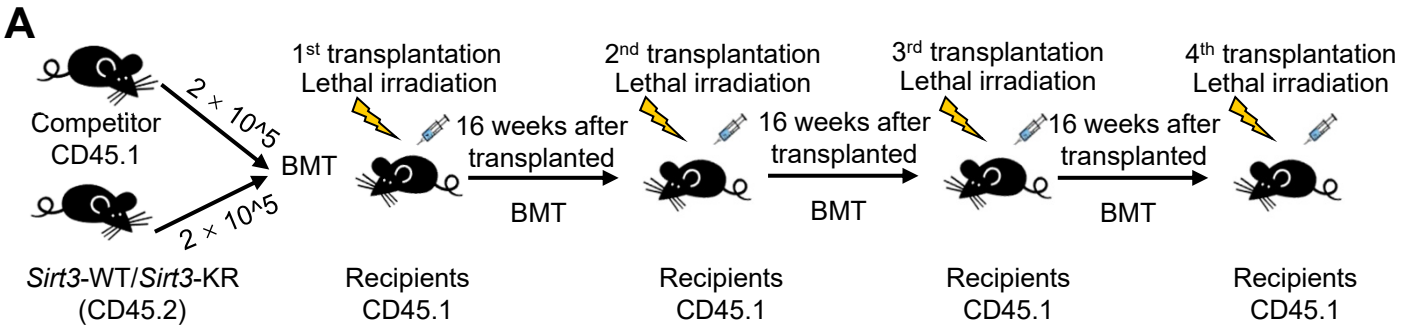
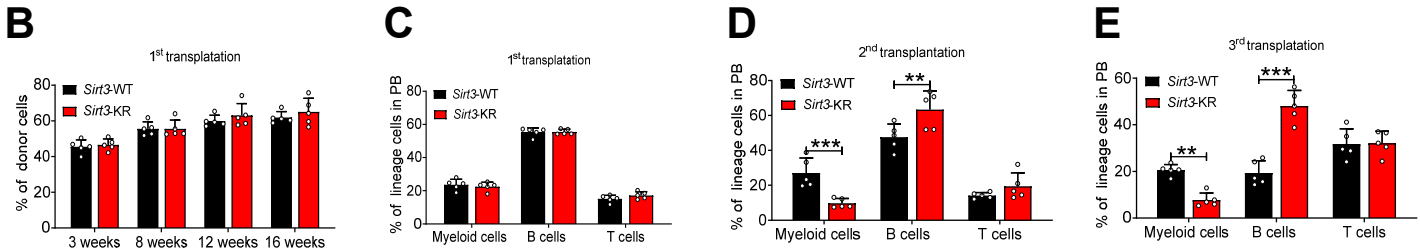
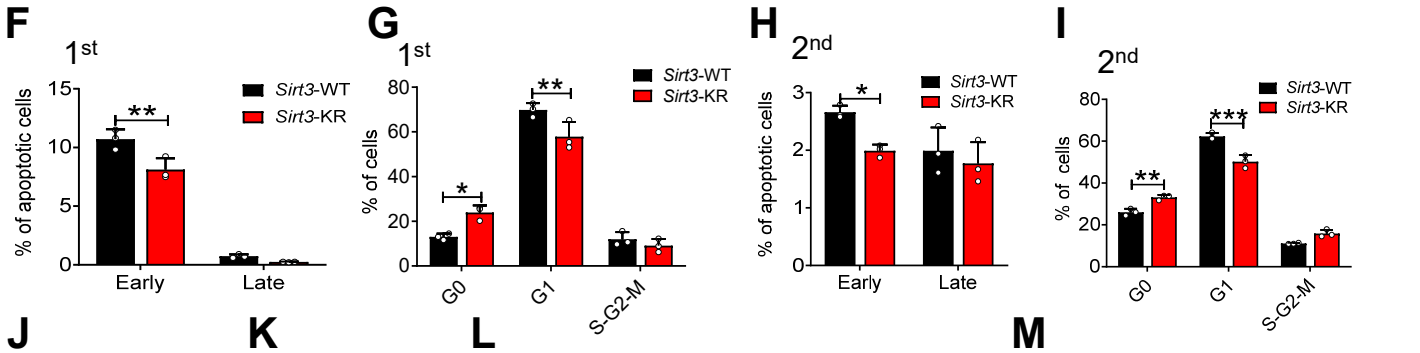

A
Sirt3-WT
Sirt3-Het
Sirt3-KR
B
HSC frequency (%)
Sirt3-WT
Sirt3-KR
young
old
C
% of lineage cell in BM
Myeloid cells
B cells
T cells
young
old
D
young
old
Lin- cells
HSCs
E
% SA-β-Gal positive cells
Lin- cells
HSCs
F
Sirt3-WT
or
Sirt3-KR
BMT
2×10^6
per mice
Lethal irradiation
Recipients
1. HSC frequency;
2. Lineage distributions ;
3. Lifespan;
4. Repopulation ability;
……
G
Body weight of recipients (g)
12 Weeks
14 Weeks
16 Weeks
20 Weeks
24 Weeks
28 Weeks
32 Weeks
36 Weeks
40 Weeks
44 Weeks
48 Weeks
52 Weeks
H
Body weight (g)
I
HSC frequency (%)
J
% of lineage cells in PB
Myeloid cells
B cells
T cells
K
Sirt3-old
% of donor cells
3 Weeks
8 Weeks
12 Weeks
16 Weeks

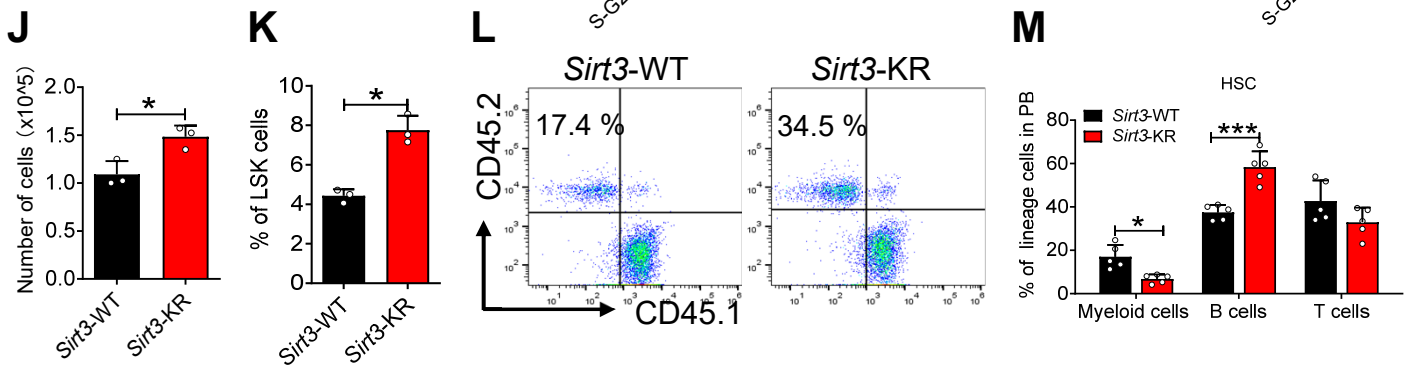
Figure S1. Related to Figure 1. SIRT3 activation inhibits HSC aging under stress conditions and markedly extends the overall lifespan of mice. A) Schematic diagram of the construction of the SIRT3 SUMOylation site mutant mouse strains. B) The frequencies of immunophenotypic $Lin^{-}Sca\text{-}1^{+}c\text{-}Kit^{+}CD34^{-}CD135^{-}$ LT-HSCs in the BM of young or old *Sirt3*-WT and *Sirt3*-KR mice were quantitated by flow cytometric analysis. C) The frequencies of myeloid cells ($Mac\text{-}1^{+}$ and $Gr\text{-}1^{+}$), B cells ($B220^{+}$) and T cells ($CD3e^{+}$) in the BM of young or old *Sirt3*-WT and *Sirt3*-KR mice were quantitated by flow cytometric analysis. D) SA-β-Gal staining of BM cells from young or old *Sirt3*-WT and *Sirt3*-KR mice are shown. Scale bar, 10 μm. E) Frequencies of SA-β-Gal cells among Lin^{-} and HSCs in the BM of young or old *Sirt3*-WT and *Sirt3*-KR mice. F) Schematic diagram of the strategy used to construct the aging model. G) Body weight of the recipient mice receiving *Sirt3*-WT or *Sirt3*-KR BM donor cells was monitored from 12 to 52 weeks. H) Body weight of recipient mice at the end stage was monitored. I) HSC frequency in recipient mice at end stage. J) Percentages of myeloid, B, and T cells in PB of recipient mice at end stage. K) The repopulation ability of donor cells from aged (24-month-old) *Sirt3*-WT and *Sirt3*-KR mice was determined by flow cytometric analysis at the indicated time points (n=5). (Each dot represents an individual mouse). *P<0.05, **P<0.01, ***P<0.001.

Figure S2


A
Competitor
CD45.1
2 × 10^5
BMT
2 × 10^5
Sirt3-WT/Sirt3-KR
(CD45.2)
1st transplantation
Lethal irradiation
16 weeks after
transplanted
BMT
Recipients
CD45.1
2nd transplantation
Lethal irradiation
16 weeks after
transplanted
BMT
Recipients
CD45.1
3rd transplantation
Lethal irradiation
16 weeks after
transplanted
BMT
Recipients
CD45.1
4th transplantation
Lethal irradiation
Recipients
CD45.1


B
1st transplatation
% of donor cells
Sirt3-WT
Sirt3-KR
3 weeks
8 weeks
12 weeks
16 weeks
C
1st transplatation
% of lineage cells in PB
Myeloid cells
B cells
T cells
D
2nd transplantation
% of lineage cells in PB
E
3rd transplatation
% of lineage cells in PB


F
1st
% of apoptotic cells
Early
Late
G
1st
% of cells
G0
G1
S-G2-M
H
2nd
% of apoptotic cells
I
2nd
% of cells


J
Number of cells (x10^5)
K
% of LSK cells
L
Sirt3-WT
Sirt3-KR
17.4 %
34.5 %
CD45.2
CD45.1
M
HSC
% of lineage cells in PB

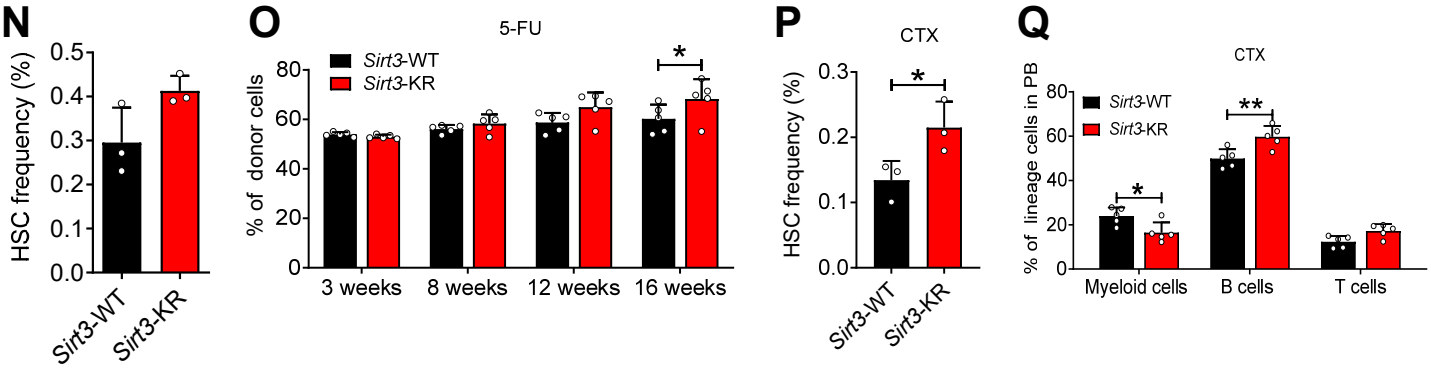

N
HSC frequency (%)
O
5-FU
% of donor cells
3 weeks
8 weeks
12 weeks
16 weeks
P
CTX
HSC frequency (%)
Q
CTX
% of lineage cells in PB

Figure S2. Related to Figure 2. The deSUMOylation of SIRT3 preserves HSC self-renewal under stress conditions. A) Schematic diagram of the strategy for serial bone marrow transplantation. B) Repopulation of *Sirt3*-WT and *Sirt3*-KR donor cells was measured 3 to 16 weeks after the 1st transplantation (n=5). C-E) Multilineage differentiation of donor cells into myeloid cells (Mac-1^{+} Gr-1^{+}), B cells (B220^{+}), and T cells (CD3^{+}) in PB was quantitated by flow cytometry at 16 weeks after the 1st (C), 2nd (D) and 3rd (E) transplantations (n=5). F-G) Frequencies of apoptotic LT-HSCs (F) and the cell cycle status of HSCs (G) derived from *Sirt3*-WT and *Sirt3*-KR donor cells were measured after the 1^{s} transplantation (n=3). H-I) Frequencies of apoptotic LT-HSCs (H) and the cell cycle status of HSCs (I) derived from *Sirt3*-WT and *Sirt3*-KR donor cells were measured after the secondary transplantation (n=3). J) Total cell numbers of cultured *Sirt3*-WT and *Sirt3*-KR HSCs after 8 days of *in vitro* culture. K) HSCs from *Sirt3*-WT and *Sirt3*-KR mice were cultured for 8 days, and the frequencies of Lin^{-}Sca-1^{+}c-Kit^{+} (LSK) cells were assessed by flow cytometric analysis (n=3). L) Representative flow cytometric analyses of the repopulation of cultured HSCs from *Sirt3*-WT and *Sirt3*-KR mice at 8 weeks post-transplantation. M) Multilineage contribution of donor cells in PB was quantified at 16 weeks after transplantation (n=5). N) Frequencies of immunophenotypic Lin^{-}Sca-1^{+}c-Kit^{+}CD34^{-}CD135^{-} LT-HSCs in the BM of *Sirt3*-WT and *Sirt3*-KR mice after 5-FU treatment (n=3). O) The repopulation of *Sirt3*-WT and *Sirt3*-KR donor cells after 5-FU treatment was measured by flow cytometry at the indicated time points after transplantation (n=5). P) Frequencies of immunophenotypic Lin^{-}Sca-1^{+}c-Kit^{+}CD34^{-}CD135^{-} LT-HSCs in the BM of *Sirt3*-WT and *Sirt3*-KR mice after cyclophosphamide (CTX) treatment (n=3). Q) The multilineage contribution of donor cells in PB was quantified at 16 weeks after CTX treatment and transplantation (n=5). *P<0.05, **P<0.01, ***P<0.001.

Figure S3

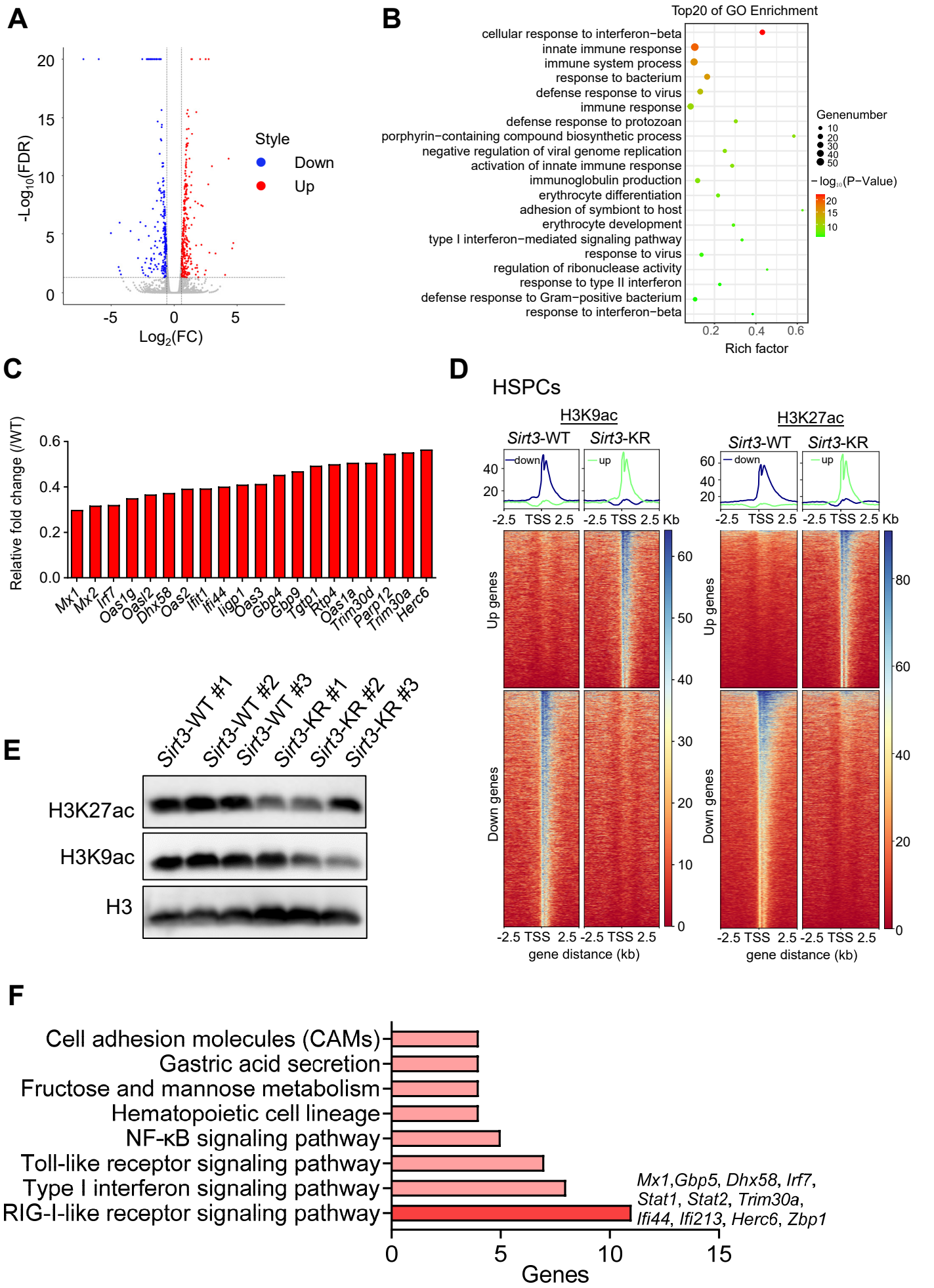

A
-Log10(FDR)
Log2(FC)
Style
Down
Up
B
Top20 of GO Enrichment
cellular response to interferon−beta
innate immune response
immune system process
response to bacterium
defense response to virus
immune response
defense response to protozoan
porphyrin−containing compound biosynthetic process
negative regulation of viral genome replication
activation of innate immune response
immunoglobulin production
erythrocyte differentiation
adhesion of symbiont to host
erythrocyte development
type I interferon−mediated signaling pathway
response to virus
regulation of ribonuclease activity
response to type II interferon
defense response to Gram−positive bacterium
response to interferon−beta
Rich factor
Genenumber
− log10(P−Value)
C
Relative fold change (/WT)
Mx1
Mx2
Irf7
Oas1g
Oasl2
Dhx58
Oas2
Ifit1
Ifi44
Iigp1
Oas3
Gbp4
Gbp9
Tgtp1
Rtp4
Oas1a
Trim30d
Parp12
Trim30a
Herc6
D
HSPCs
H3K9ac
H3K27ac
Sirt3-WT
Sirt3-KR
down
up
Up genes
Down genes
gene distance (kb)
E
Sirt3-WT #1
Sirt3-WT #2
Sirt3-WT #3
Sirt3-KR #1
Sirt3-KR #2
Sirt3-KR #3
H3K27ac
H3K9ac
H3
F
Cell adhesion molecules (CAMs)
Gastric acid secretion
Fructose and mannose metabolism
Hematopoietic cell lineage
NF-κB signaling pathway
Toll-like receptor signaling pathway
Type I interferon signaling pathway
RIG-I-like receptor signaling pathway
Mx1,Gbp5, Dhx58, Irf7,
Stat1, Stat2, Trim30a,
Ifi44, Ifi213, Herc6, Zbp1
Genes

Figure S3. Related to Figure 3. SIRT3 negatively regulates target genes in the RIG-1 signaling pathway by deacetylating H3K9ac and H3K27ac in HSCs. A) Volcano plots showing differentially expressed genes in *Sirt3*-WT and *Sirt3*-KR HSCs. A total of 305 genes were significantly upregulated, whereas 288 genes were downregulated in *Sirt3*-KR HSCs. B) Changes in pathways in HSCs from *Sirt3*-WT and *Sirt3*-KR mice evaluated by RNA-sequencing (RNA-seq) analyses. C) The downregulated expression of potential candidate genes related to signaling pathways involved in the inflammatory response in *Sirt3*-KR HSCs (compared with *Sirt3*-WT HSCs) were analyzed by RNA-seq. D) Heatmap showing CUT&Tag-seq coverage at sites with altered H3K9ac and H3K27ac modifications in *Sirt3*-WT and *Sirt3*-KR hematopoietic stem/progenitor cells (HSPCs). E) The levels of H3K9ac and H3K27ac in *Sirt3*-WT and *Sirt3*-KR HSPCs were determined by western blotting. F) KEGG enrichment analysis of the 90 commonly downregulated genes in *Sirt3*-KR HSCs identified by RNA-seq and H3K9ac/H3K27ac CUT&Tag, showing the top 8 enriched pathways. The x-axis represents the number of genes enriched in each pathway.

Figure S4

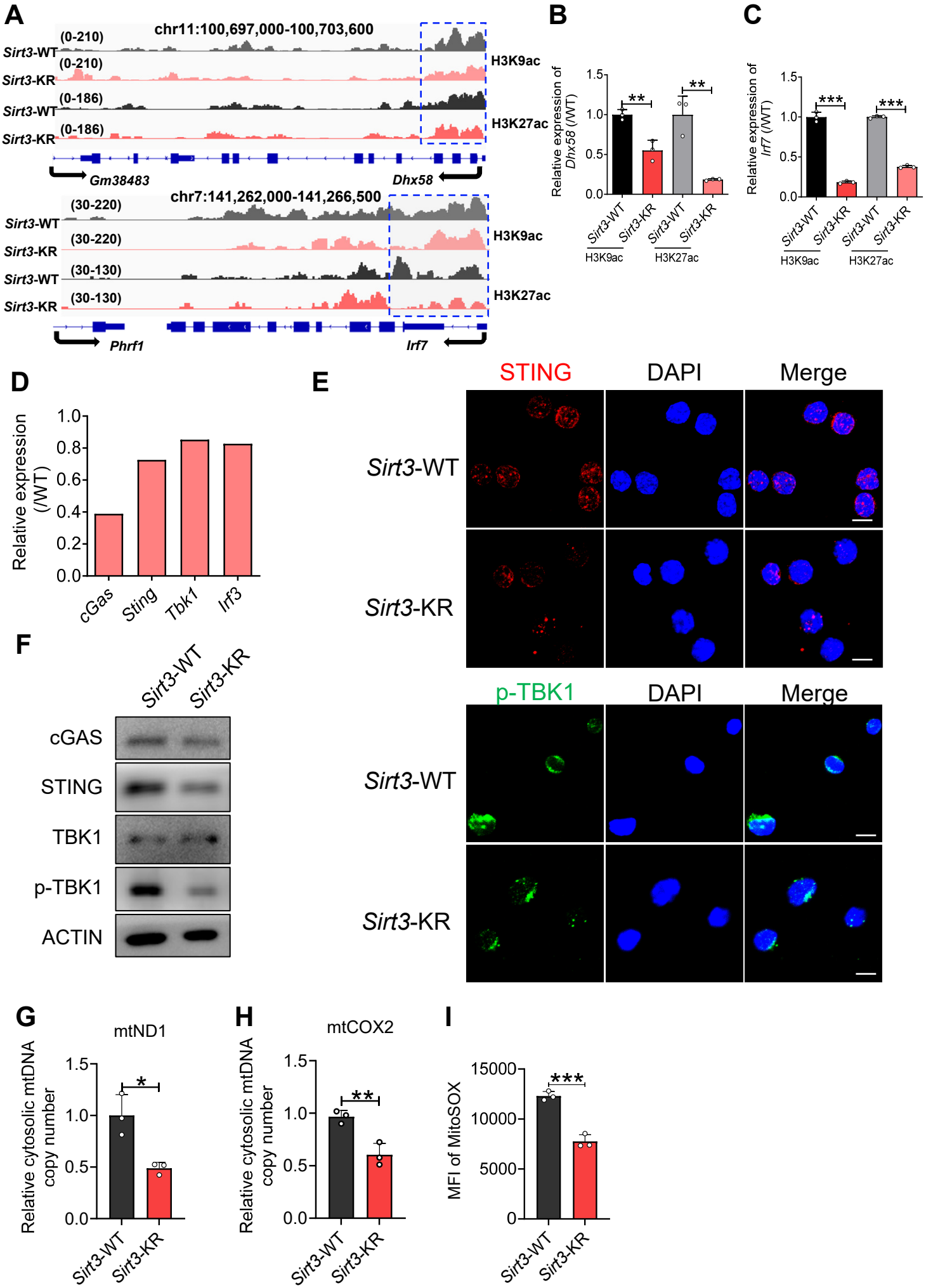

A
chr11:100,697,000-100,703,600
(0-210)
Sirt3-WT
(0-210)
Sirt3-KR
(0-186)
Sirt3-WT
(0-186)
Sirt3-KR
H3K9ac
H3K27ac
Gm38483
Dhx58
chr7:141,262,000-141,266,500
(30-220)
Sirt3-WT
(30-220)
Sirt3-KR
(30-130)
Sirt3-WT
(30-130)
Sirt3-KR
H3K9ac
H3K27ac
Phrf1
Irf7
B
Relative expression of Dhx58 (/WT)
Sirt3-WT
Sirt3-KR
Sirt3-WT
Sirt3-KR
H3K9ac
H3K27ac
C
Relative expression of Irf7 (/WT)
Sirt3-WT
Sirt3-KR
Sirt3-WT
Sirt3-KR
H3K9ac
H3K27ac
D
Relative expression (/WT)
cGas
Sting
Tbk1
Irf3
E
STING
DAPI
Merge
Sirt3-WT
Sirt3-KR
p-TBK1
DAPI
Merge
Sirt3-WT
Sirt3-KR
F
Sirt3-WT
Sirt3-KR
cGAS
STING
TBK1
p-TBK1
ACTIN
G
mtND1
Relative cytosolic mtDNA copy number
Sirt3-WT
Sirt3-KR
H
mtCOX2
Relative cytosolic mtDNA copy number
Sirt3-WT
Sirt3-KR
I
MFI of MitoSOX
Sirt3-WT
Sirt3-KR

Figure S4. Related to Figure 3. SIRT3 sustains HSC activities and delays aging by regulating inflammation-associated pathways. A) Analysis of H3K9ac and H3K27ac CUT&Tag-seq at peaks in the genomic regions of DHX58 and IRF7. B) ChIP-qPCR analysis of the H3K9ac and H3K27ac levels at the *Dhx58* promoter in *Sirt3*-WT and *Sirt3*-KR HSPCs. C) ChIP-qPCR analysis of the H3K9ac and H3K27ac levels at the *Irf7* promoter in *Sirt3*-WT and *Sirt3*-KR HSPCs. D) The relative expression levels of candidate genes related to the cGAS-STING signaling pathway in *Sirt3*-KR HSCs are shown (compared to that of *Sirt3*-WT HSCs). E) Immunofluorescence staining showing STING and p-TBK1 levels in *Sirt3*-WT and *Sirt3*-KR HSCs. Scale bar, 10 μm. F) The levels of cGAS, STING, TBK1 and p-TBK1 in *Sirt3*-WT and *Sirt3*-KR HSCs were determined by western blotting. G-H) Relative copy number of cytosolic mtDNA (*mtND1*, G; *mtCOX2*, H) in *Sirt3*-WT and *Sirt3*-KR HSPCs. I) Mean fluorescence intensity (MFI) of MitoSOX in *Sirt3*-WT and *Sirt3*-KR HSCs. *P<0.05, **P<0.01, ***P<0.001.

Figure S5

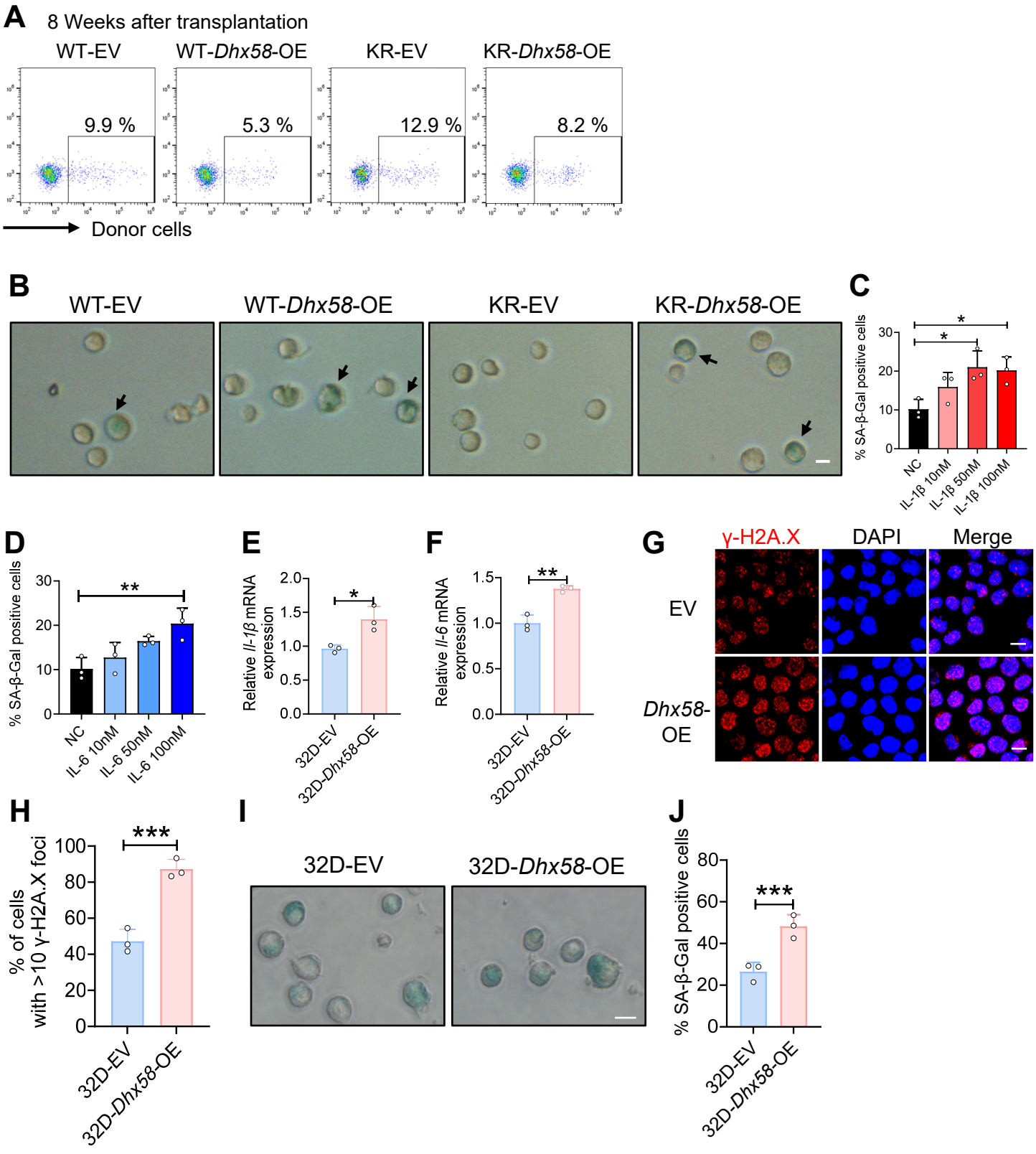

A
8 Weeks after transplantation
WT-EV
WT-Dhx58-OE
KR-EV
KR-Dhx58-OE
9.9 %
5.3 %
12.9 %
8.2 %
Donor cells
B
WT-EV
WT-Dhx58-OE
KR-EV
KR-Dhx58-OE
C
% SA-β-Gal positive cells
NC
IL-1β 10nM
IL-1β 50nM
IL-1β 100nM
D
% SA-β-Gal positive cells
NC
IL-6 10nM
IL-6 50nM
IL-6 100nM
E
Relative Il-1β mRNA expression
32D-EV
32D-Dhx58-OE
F
Relative Il-6 mRNA expression
32D-EV
32D-Dhx58-OE
G
γ-H2A.X
DAPI
Merge
EV
Dhx58-OE
H
% of cells with >10 γ-H2A.X foci
32D-EV
32D-Dhx58-OE
I
32D-EV
32D-Dhx58-OE
J
% SA-β-Gal positive cells
32D-EV
32D-Dhx58-OE

Figure S5. Related to Figure 4. SIRT3 promotes HSC self-renewal and delays HSC aging through the downregulation of DHX58. A) Representative flow cytometric analyses of the repopulation of HSCs from *Sirt3*-WT and *Sirt3*-KR mice with/without *Dhx58* overexpression (RFP^+ cells) at 8 weeks post-transplantation. B) Representative images of SA-β-Gal-stained BM cells from *Sirt3*-WT, *Sirt3*-KR, *Dhx58*-overexpressing *Sirt3*-WT or *Sirt3*-KR. Scale bar, 10 μm. C-D) Percentages of SA-β-Gal-positive 32D cells after treatment with different doses of IL-1β (C) or IL-6 (D) for 7 days (n=3). E-F) The relative mRNA levels of *Il-1β* (E) and *Il-6* (F) in 32D cells with/without overexpression of *Dhx58* were measured by qRT-PCR (n=3). G) Immunofluorescence staining showing γ-H_2A.X levels in 32D cells with/without overexpression of *Dhx58*. Scale bar, 10 μm. H) The proportions of cells with more than 10 γ-H2A.X foci in G were calculated (n=3). I) Representative SA-β-Gal staining of 32D cells with/without overexpression of *Dhx58* is shown. Scale bar, 10 μm. J) The percentage of SA-β-Gal-positive 32D cells with/without overexpression of *Dhx58* (n=3). *P<0.05, **P<0.01, ***P<0.001.

Figure S6

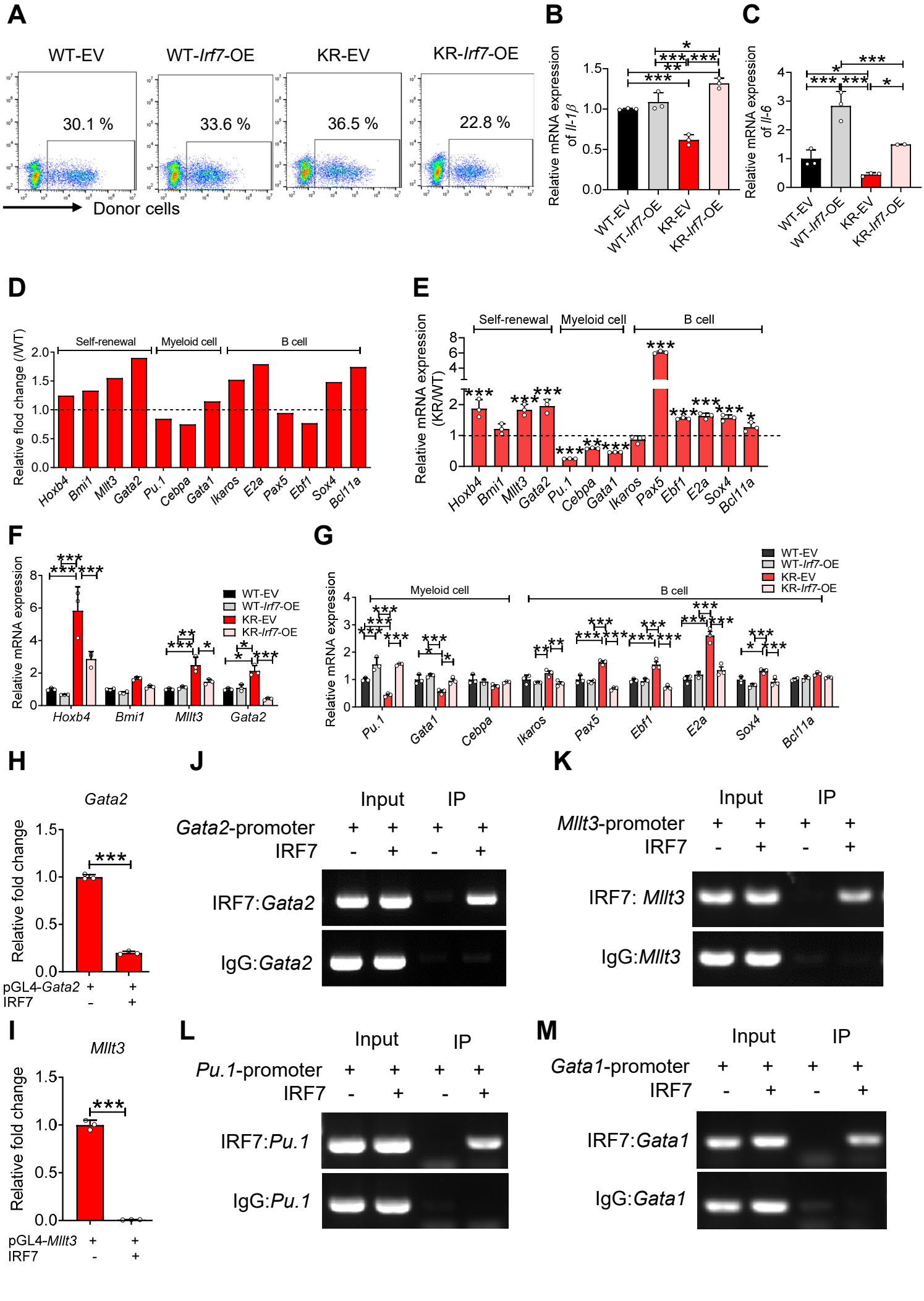

A
WT-EV
WT-Irf7-OE
KR-EV
KR-Irf7-OE
30.1 %
33.6 %
36.5 %
22.8 %
Donor cells
B
Relative mRNA expression of Il-1β
C
Relative mRNA expression of Il-6
D
Relative flod change (/WT)
Self-renewal
Myeloid cell
B cell
Hoxb4
Bmi1
Mllt3
Gata2
Pu.1
Cebpa
Gata1
Ikaros
E2a
Pax5
Ebf1
Sox4
Bcl11a
E
Relative mRNA expression (KR/WT)
F
Relative mRNA expression
WT-EV
WT-Irf7-OE
KR-EV
KR-Irf7-OE
G
H
Gata2
Relative fold change
pGL4-Gata2
IRF7
J
Input
IP
Gata2-promoter
IRF7
IRF7:Gata2
IgG:Gata2
K
Mllt3-promoter
IRF7: Mllt3
IgG:Mllt3
I
Mllt3
pGL4-Mllt3
L
Pu.1-promoter
IRF7:Pu.1
IgG:Pu.1
M
Gata1-promoter
IRF7:Gata1
IgG:Gata1

Figure S6. Related to Figure 5. IRF7 serves as a DHX58 downstream target to regulate HSC stemness and aging. A) Representative flow cytometric analyses of the repopulation of HSCs from *Sirt3*-WT and *Sirt3*-KR mice with/without *Irf7* overexpression (RFP^+ cells). B-C) The relative mRNA levels of the senescence-associated secretory phenotypes (SASP) genes *Il-1β* (B) and *Il-6* (C) were measured in *Sirt3*-WT, *Sirt3*-KR, *Irf7*-overexpressing *Sirt3*-WT or *Sirt3*-KR HSCs by qRT-PCR (n=3). D) The relative expression levels of candidate genes related to self-renewal and lineage differentiation in *Sirt3*-KR HSCs (compared with *Sirt3*-WT HSCs) were analyzed by RNA-seq. E) The relative mRNA expression levels of self-renewal-related and lineage differentiation-related genes in *Sirt3*-KR HSCs (compared with *Sirt3*-WT HSCs) were determined by qRT-PCR (n=3). F) The relative mRNA expression of self-renewal-related candidate genes in *Sirt3*-WT, *Sirt3*-KR, and *Irf7*-overexpressing *Sirt3*-WT or *Sirt3*-KR HSCs determined by qRT-PCR (n=3). G) The relative mRNA expression of lineage differentiation-related candidate genes in *Sirt3*-WT, *Sirt3*-KR, *Irf7*-overexpressing *Sirt3*-WT or *Sirt3*-KR HSCs determined by qRT-PCR (n=3). H-I) A luciferase reporter assay was performed to evaluate the transcriptional activity of IRF7 at the promoters of *Gata2* (H) and *Mllt3* (I) (n=3). J-M) The binding of IRF7 to the *Gata2* (J), *Mllt3* (K), *Pu.1* (L) and *Gata1* (M) promoter regions was determined by a ChIP assay. *P<0.05, **P<0.01, ***P<0.001.

Figure S7

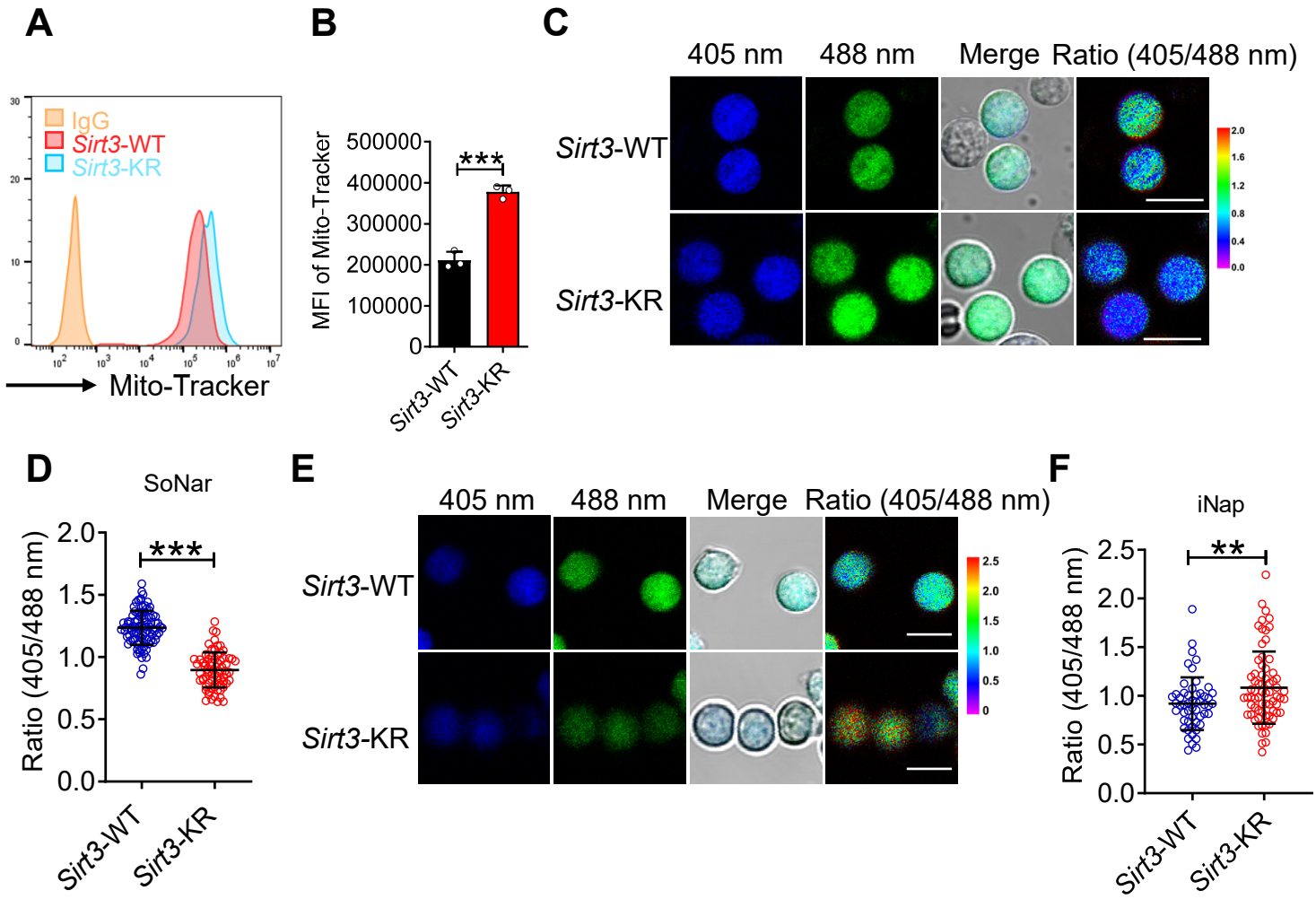

A
IgG
Sirt3-WT
Sirt3-KR
Mito-Tracker
B
MFI of Mito-Tracker
***
Sirt3-WT
Sirt3-KR
C
405 nm
488 nm
Merge
Ratio (405/488 nm)
Sirt3-WT
Sirt3-KR
D
SoNar
Ratio (405/488 nm)
***
Sirt3-WT
Sirt3-KR
E
405 nm
488 nm
Merge
Ratio (405/488 nm)
Sirt3-WT
Sirt3-KR
F
iNap
Ratio (405/488 nm)
**
Sirt3-WT
Sirt3-KR
G
Anti-Oxidative related genes
Glycolysis
Oxidative phosphorylation
PPP
Relative mRNA expression (/WT)
Sod1
Sod2
Txn1
Prdx1
Prdx2
Prdx3
Prdx4
Prdx5
Prdx6
Gpx1
Gpx2
Gpx3
Txnrd1
Txnrd2
Txnrd3
Txndc17
Glrx1
Glrx2
Glrx3
Nox1
Nox2
Gsr
Glut2
Glut3
Glut4
Hk1
Pfkl
Pfkm
Gapdh
Pkm2
Ldha
Mdh1
Mdh2
Idh1
Idh2
Idh3a
Idh3b
Idh3g
Aco2
Atp5i
Atp5o
Cox6b1
Cox18
Ndufb5
G6pd
Pgd

Figure S7. Related to Figure 6. SIRT3 enhances mitochondrial metabolism and α-KG generation in HSCs. A) Representative flow cytometric analyses of Mito-Tracker staining in *Sirt3*-WT and *Sirt3*-KR HSCs. B) Quantification data of the Mito-Tracker MFI in *Sirt3*-WT and *Sirt3*-KR HSCs at panel A (n=3). C) Representative images of the fluorescence ratios (F_{405}/F_{488} nm) in the HSCs derived from *Sirt3*-WT-SoNar and *Sirt3*-KR-SoNar mice. Scale bar, 10 μm. D) Quantification of the SoNar fluorescence ratio (F_{405}/F_{488} nm) in the HSCs of *Sirt3*-WT-SoNar and *Sirt3*-KR-SoNar mice in panel C (WT: n=98; KR: n=76). E) Representative images of the fluorescence ratio (F_{405}/F_{488} nm) in the HSCs of *Sirt3*-WT-iNap and *Sirt3*-KR-iNap mice. Scale bar, 10 μm. F) Quantification of the iNap fluorescence ratio (F_{405}/F_{488} nm) in the HSCs of *Sirt3*-WT-iNap and *Sirt3*-KR-iNap mice in panel E (WT: n=53; KR: n=70). G) The relative mRNA expression levels of redox homeostasis-related, glycolysis and oxidative phosphorylation related candidate genes in *Sirt3*-WT and *Sirt3*-KR HSCs were determined by qRT-PCR (n=3). *P<0.05, **P<0.01, ***P<0.001.

Supplemental Methods and Materials

Animals

Sirt3-K223R mutant mice (*Sirt3*-KR) were obtained from Dr. Jinke Cheng's Laboratory (Shanghai Jiao Tong University, China). CD45.1 mice were provided by Dr. Jiang Zhu at Ruijin Hospital, Shanghai, China. For all experiments, 6- to 8-week-old C57BL/6 CD45.2 mice were ordered from the Shanghai SLAC Laboratory Animal Company (Shanghai, China) and maintained at the Animal Core Facility at Shanghai Jiao Tong University School of Medicine.

Competitive reconstitution analysis

For the analysis of the function of SIRT3 in HSC activities, a serial competitive reconstitution analysis was performed with *Sirt3*-WT or *Sirt3*-KR mice, and a total of 2×10^5 *Sirt3*-WT or *Sirt3*-KR CD45.2 donor bone marrow (BM) cells were mixed with 2×10^5 CD45.1 competitor BM cells and transplanted into lethally irradiated CD45.1 recipient mice by retroorbital injection.

In other stress conditions, $Lin^-Sca1^+c\text{-}Kit^+CD34^-CD135^-$ LT-HSCs were sorted from *Sirt3*-WT and *Sirt3*-KR mice, cultured for 8 days *in vitro*, and then injected into lethally irradiated recipient mice along with 2×10^5 CD45.1 competitor cells. In some cases, six-week-old *Sirt3*-WT and *Sirt3*-KR mice were treated with 200 mg/kg cyclophosphamide (CTX) for 4 weeks or with 150 mg/kg 5-fluorouracil (5-FU) for 6 days through intraperitoneal injection. Then, 2×10^5 *Sirt3*-WT or *Sirt3*-KR BM cells together with 3×10^5 CD45.1 competitors were transplanted into lethally irradiated CD45.1 mice.

For the rescue experiments, the retroviral XZ201-*Dhx58*-HA-mCherry-expressing plasmid, XZ201-*Irf7*-HA-mCherry or empty vector was mixed with the pCL-ECO

packaging plasmid at a ratio of 2:1 and transfected into 293T cells. The virus-containing supernatant was harvested for the infection of lineage-negative (Lin^{-}) cells isolated from *Sirt3*-WT or *Sirt3*-KR mice, which were preconditioned with 100 mg/kg 5-FU for 6 days. The infected cells were then coinjected into lethally irradiated recipient mice along with 2×10^5 CD45.1 competitor cells to ensure a competitive environment. The recipient mice were analyzed for the repopulation of CD45.2 donor cells at 3 to 16 weeks after transplantation. The number of hematologic cells in the peripheral blood (PB) was also evaluated 16 weeks after transplantation.

Flow cytometry

The frequency of LT-HSCs was evaluated by freshly isolating *Sirt3*-WT or *Sirt3*-KR BM cells and subjecting them to a flow cytometric analysis. Immunophenotypic Lin^- $Sca\text{-}1^+c\text{-}Kit^+CD135^-CD34^-$ LT-HSCs were evaluated or FACS-purified by staining with a biotinylated lineage cocktail (anti-CD3, anti-B220, anti-Mac-1, anti-Gr-1, and anti-Ter119 antibodies; BD Pharmingen), followed by incubation with streptavidin-PE/Cy5.5, anti-Sca-1-FITC, anti-c-Kit-APC, anti-Flk-2-eFluo450 (anti-CD135-eFluo450) and anti-CD34-PE antibodies (eBioscience). For the analysis of the repopulation ability of HSCs, the PB of recipient mice was collected, followed by the lysis of red blood cells and staining with anti-CD45.2-FITC, anti-CD45.1-PE, anti-CD3e-APC (for the T-lymphoid lineage), anti-B220-PE (for the B-lymphoid lineage), anti-Mac-1-APC, or anti-Gr-1-PE monoclonal antibodies (eBioscience; cells co-stained with anti-Mac-1 and anti-Gr-1 were deemed to be of the myeloid lineage). The cell cycle or apoptotic status was measured in purified LT-HSCs with Hoechst 33342/Pyronin Y or anti-Annexin V-PE/7-AAD (BD Pharmingen), followed by a flow cytometric analysis. Mitochondrial membrane potential and reactive oxygen species

(ROS) levels were assessed in purified LT-HSCs. For mitochondrial membrane potential measurement, cells were stained with 5 nM Tetramethylrhodamine (TMRM, Sigma) at 37 °C for 30 min. For ROS detection, cells were incubated with 5 μM 2',7'-dichlorodihydrofluorescein diacetate (H_2DCFDA, Invitrogen) at 37 °C for 30 min. After staining, cells were washed and resuspended in PBS, followed by flow cytometric analysis.

Cell culture

Immunophenotypic $Lin^-Sca\text{-}1^+c\text{-}Kit^+CD135^-CD34^-$ LT-HSCs or Lin^- cells were cultured with StemSpan serum-free medium (StemCell Technologies) supplemented with 10 ng/mL mouse SCF, 20 ng/mL mouse TPO, and 10 ng/mL FLT3-L (Peprotech) in a U-bottom 96-well plate. For the DHX58 or IRF7 overexpression experiments, the XZ201-*Dhx58*-HA-mCherry, XZ201-*Irf7*-HA-mCherry, or empty vector was cotransfected into 293T cells with the packaging plasmid pCL-ECO (2:1). The supernatant was collected at 48-72 h after transfection. Lin^- cells from *Sirt3*-WT or *Sirt3*-KR mice and 32D cells were infected with the retrovirus in the presence of 4 μg/mL polybrene, centrifuged at 800×g for 2 h, and then cultured for 48 h. RFP^+ 32D cells and RFP^+ Lin^- BM cells were sorted by FACS.

RNA-seq and quantitative RT-PCR

Sirt3-WT or *Sirt3*-KR $Lin^-Sca\text{-}1^+c\text{-}Kit^+CD135^-CD34^-$ LT-HSCs were sorted by flow cytometry, total RNA was extracted, and the samples were subjected to RNA sequencing at Shanghai Lie Bing Biomedical Technology Co., Ltd. A Gene Ontology enrichment analysis was performed with the Bioconductor package top GO. The analyses of enriched KEGG pathways were conducted using the Bioconductor package

GSEA. The candidate genes were further validated in *Sirt3*-WT or *Sirt3*-KR HSCs by quantitative RT-PCR. Briefly, first-strand cDNA was reverse transcribed using AMV reverse transcriptase (TaKaRa). RT-PCRs were performed according to the manufacturer's protocol with an Applied Biosystems 7900HT instrument. The mRNA levels were normalized to the level of β-actin RNA transcripts. The sequences of primers used are shown in Table S1.

β-galactosidase staining for senescence

The senescence of BM cells or 32D cells was performed with a senescence-associated β-galactosidase staining kit (Yeasen) according to the manufacturer's instructions. Briefly, the cells were fixed with fixative buffer for 15 min. After washes with PBS, the fixed cells were stained with fresh SA-β-Gal staining solution and incubated at 37 ℃ for 16 h. Images were acquired using an inverted fluorescence microscope (Nikon).

Immunofluorescence staining

For the immunofluorescence staining, *Sirt3*-WT or *Sirt3*-KR HSCs were sorted by flow cytometry and fixed with methyl alcohol at 4 °C for 15 min. The fixed cells were washed 3 times with PBS for 10 min each, permeabilized with a 0.1% Triton X-100 solution at room temperature for 15 min and blocked with 5% bovine serum albumin (Sigma) at room temperature for 1 h. The cells were then stained with γ-H2A.X (Abcam), p-TBK1 (Cell Signaling Technology), or STING (Cell Signaling Technology) antibodies at 4 °C overnight. The sections were then washed with PBS and incubated with the appropriate Alexa Fluor 488-conjugated secondary antibody (Thermo Fisher Scientific) or Alexa Fluor 555-conjugated secondary antibody (Thermo Fisher Scientific) at room temperature for 1 h. Nuclei were counterstained with DAPI (Thermo

Fisher Scientific) before imaging. Images were obtained with a Nikon A1 confocal microscope.

Luciferase reporter assay

The luciferase reporter vector pGL4.27 containing the promoter was constructed to identify the transcriptional regulation of *Gata2, Mllt3, Gata1* and *Pu.1* by IRF7. The indicated concentrations of the pLVX-*Irf7*-strepII-GFP (or negative control vector) were cotransfected with pGL4.27 promoter reporter vectors into 293T cells. Luciferase activities were measured using a luciferase reporter system (GloMax® Multi Instrument) 24 h after transfection. Relative luciferase activity was calculated as the ratio of firefly luciferase to Renilla luciferase activity.

Chromatin immunoprecipitation (ChIP) assays

ChIP assays were performed using a ChIP Assay Kit (Beyotime, P2078). 293T cells were cotransfected with pLVX-*Irf7*-strepII-GFP and pGL4.27-*Gata2*-promoter, pGL4.27-*Mllt3*-promoter, pGL4.27-*Gata1*-promoter or pGL4.27-*Pu.1*-promoter, crosslinked with 1% formaldehyde (Sigma) at 37 °C for 10 min, and then incubated with anti-IRF7 antibodies (Cell Signaling Technology) or rabbit control IgG (Cell Signaling Technology) at 4 °C overnight. For the sample input, 1% of the sonicated precleared DNA was purified at the same time as the precipitated immune complex. The ChIP samples were purified with a Gel and PCR Clean-up Kit (Nucleospin). The IRF7-binding sequence was amplified by semiquantitative PCR using primers specific for the *Gata2, Mllt3, Gata1* or *Pu.1* promoter region, as listed in Table S1.

Western blotting

Lysates of FACS-purified BM cells or cell lines were electrophoresed on 10% SDS polyacrylamide gels and transferred onto PVDF membranes (Millipore). The membranes were blocked with 5% nonfat milk and then incubated with an appropriate antibody, followed by an incubation with an HRP-conjugated secondary antibody. For the detection of acetylation, the protein was incubated with H3K27ac (Cell Signaling Technology), H3K9ac (Cell Signaling Technology), or H3 (Cell Signaling Technology) antibodies.

Cleavage under targets and tagmentation (CUT&Tag) analyses

The CUT&Tag assay was conducted using the NovoNGS CUT&Tag 3.0 High-Sensitivity Kit (Novoprotein). Briefly, isolated *Sirt3*-WT or *Sirt3*-KR $Lin^{-}Sca\text{-}1^{+}c\text{-}Kit^{+}CD135^{-}CD34^{-}$ LT-HSCs were enriched with ConA beads and resuspended in primary antibody buffer containing the H3K9ac antibody or H3K27ac antibody. The suspension was then incubated overnight at 4 °C. Next, secondary antibody buffer containing the anti-rabbit IgG antibody (Abcam) was added, and the mixture was incubated for 1 h. The beads were washed three times with antibody buffer and subsequently incubated with the Protein A/G-Tn5 transposome for 1 h. The beads were resuspended in tagmentation buffer (10 mM $MgCl_2$ in ChiTaq buffer) and incubated at 37 °C for 1 h. The incubation was terminated by the addition of 10% SDS and an incubation at 55 °C for 10 min. DNA fragments were extracted using Tagment DNA extraction beads, and the libraries were amplified using 5x AmpliMix. The DNA libraries were further purified using DNA clean beads in preparation for sequencing and PCR. The H3K9ac or H3K27ac-binding sequence was amplified by semiquantitative PCR using primers specific for the *Irf7* and *Dhx58* promoter regions, as listed in Table S1.

Table S1. List of primer

Genotyping primers	**Sequences**
Sirt3-F	GGGACCATTACAGAGTGAAGA
Sirt3-R	CATACAGAGCCACAGACATACC
q-PCR primers	**Sequences**
Mouse-*P16*-F	ACATCAAGACATCGTGCGATATT
Mouse-*P16*-R	CCAGCGGTACACAAAGACCA
Mouse-*P21*-F	CGAGAACGGTGGAACTTTGAC
Mouse-*P21*-R	CCAGGGCTCAGGTAGACCTT
Mouse-*Mx1*-F	CCTCCCACATCTGTAAATCACTG
Mouse-*Mx1*-R	CGGTTTCCTGTGCTTGTATCA
Mouse-*Irf7*-F	CCCCAGCCGGTGATCTTTC
Mouse-*Irf7*-R	CACAGTGACGGTCCTCGAAG
Mouse-*Oas3*-F	TCTGGGGTCGCTAAACATCAC
Mouse-*Oas3*-R	GATGACGAGTTCGACATCGGT
Mouse-*Dhx58*-F	GGAAGTGATCTTACCTGCTCTGG
Mouse-*Dhx58*-R	TTGCCTCTGTCTACCGTCTCT
Mouse-*Gbp5*-F	CAGACCTATTTGAACGCCAAAGA
Mouse-*Gbp5*-R	TGCCTTGATTCTATCAGCCTCT
Mouse-*Trim30a*-F	AGAGTTGACTGGGAGAACCAA
Mouse-*Trim30a*-R	TGCAGCATTTCTAAGGTTGAGAG
Mouse-*Oas1g*-F	ATGGAGCACGGACTCAGGA
Mouse-*Oas1g*-R	TCACACACGACATTGACGGC
Mouse-*Pik3ap1*-F	TGGTCCCGGATGCCTCTTT
Mouse-*Pik3ap1*-R	CACAAGTCATTTCCTGCCAGT

Mouse-*Tlr4*-F	GCCTTTCAGGGAATTAAGCTCC
Mouse-*Tlr4*-R	GATCAACCGATGGACGTGTAAA
Mouse-*Ifit44*-F	CCTGGTTCAGCAAACACGAGT
Mouse-*Ifit44*-R	TGGCCTTGATGGAATATGTCCT
Mouse-*Parp14*-F	CTGTATCAGCCACCGCTCAAA
Mouse-*Parp14*-R	CAACCAGTGCCGAACTCTCTT
Mouse-*Csf1*-F	GGCTTGGCTTGGGATGATTCT
Mouse-*Csf1*-R	GAGGGTCTGGCAGGTACTC
Mouse-*Ly9*-F	GCCTCAGATCATCGTGGAATC
Mouse-*Ly9*-R	TTGCAGGTATAGGGTAGGTCG
Mouse-*Il-1β*-F	GAAATGCCACCTTTTGACAGTG
Mouse-*Il-1β*-R	TGGATGCTCTCATCAGGACAG
Mouse-*Il-6*-F	CTGCAAGAGACTTCCATCCAG
Mouse-*Il-6*-R	AGTGGTATAGACAGGTCTGTTGG
Mouse-*Hoxb4*-F	CAGAGCGATTACCTACCCAGC
Mouse-*Hoxb4*-R	ATTGGGGTTTACCGTGCTCAC
Mouse-*Bmi1*-F	GCCCCTACCTCCCTACAGAC
Mouse-*Bmi1*-R	GTTGAACTCGTCTCCGATCC
Mouse-*Mllt3*-F	TGGTGAATGTGACAAGGCATATC
Mouse-*Mllt3*-R	TGTCCAGCGAGCAAAGATCAA
Mouse-*Gata2*-F	CGACGAGGTGGATGTCTTCT
Mouse-*Gata2*-R	GCTGTGCAACAAGTGTGGTC
Mouse-*Pu.1*-F	ATGTTACAGGCGTGCAAAATGG
Mouse-*Pu.1*-R	TGATCGCTATGGCTTTCTCCA
Mouse-*Gata1*-F	GATGGAATCCAGACGAGGAA

Mouse-*Gata1*-R	ACAGGCCCTGACAGTACCAC
Mouse-*Cebpa*-F	CAAGAACAGCAACGAGTACCG
Mouse-*Cebpa*-R	GTCACTGGTCAACTCCAGCAC
Mouse-*Ikaros*-F	CTCGGCCATTCGTACATGGAA
Mouse-*Ikaros*-R	GGATACCTCTGCACCGTAGC
Mouse-*Pax5*-F	TCCCAGATGTAGTCCGCCAAA
Mouse-*Pax5*-R	TCCTGTCTCATAATACCTGCCAA
Mouse-*Ebf1*-F	GTCACCACAAGCATGAATGG
Mouse-*Ebf1*-R	TCTGACAACTGGTGCGAAAG
Mouse-*E2a*-F	GGGTGCCAGCGAGATCAAG
Mouse-*E2a*-R	ATGAGCAGTTTGGTCTGCGG
Mouse-*Sox4*-F	GACCTGCTCGACCTGAACC
Mouse-*Sox4*-R	ACTCCAGCCAATCTCCCGA
Mouse-*Bcl11a*-F	GCTGTGCAACTATGCCTGTG
Mouse-*Bcl11a*-R	ACTCGATCACTGTGCCATTTTT
Mouse-*Sod1*-F	AACCAGTTGTGTTGTCAGGAC
Mouse-*Sod1*-R	CCACCATGTTTCTTAGAGTGAGG
Mouse-*Sod2*-F	CAGACCTGCCTTACGACTATGG
Mouse-*Sod2*-R	CTCGGTGGCGTTGAGATTGTT
Mouse-*Txn1*-F	CATGCCGACCTTCCAGTTTTA
Mouse-*Txn1*-R	TTTCCTTGTTAGCACCGGAGA
Mouse-*Prdx1*-F	AATGCAAAAATTGGGTATCCTGC
Mouse-*Prdx1*-R	CGTGGGACACACAAAAGTAAAGT
Mouse-*Prdx2*-F	GGTAACGCGCAAATCGGAAAG
Mouse-*Prdx2*-R	TCCAGTGGGTAGAAAAAGAGGT

Mouse-*Prdx3*-F	GTCTCGACGACTTTAAGGGAAAA
Mouse-*Prdx3*-R	ACTGAAACTGCAACTACTTCACA
Mouse-*Prdx4*-F	CTCAAACTGACTGACTATCGTGG
Mouse-*Prdx4*-R	CGATCCCCAAAAGCGATGATTTC
Mouse-*Prdx5*-F	GGCTGTTCTAAGACCCACCTG
Mouse-*Prdx5*-R	GGAGCCGAACCTTGCCTTC
Mouse-*Prdx6*-F	AAGCTGTCTATCCTCTACCCTG
Mouse-*Prdx6*-R	GTGGGAACTACCATCACGCT
Mouse-*Gpx1*-F	AGTCCACCGTGTATGCCTTCT
Mouse-*Gpx1*-R	GAGACGCGACATTCTCAATGA
Mouse-*Gpx2*-F	GCCTCAAGTATGTCCGACCTG
Mouse-*Gpx2*-R	GGAGAACGGGTCATCATAAGGG
Mouse-*Gpx3*-F	CCTTTTAAGCAGTATGCAGGCA
Mouse-*Gpx3*-R	CAAGCCAAATGGCCCAAGTT
Mouse-*Txnrd1*-F	CCCACTTGCCCCAACTGTT
Mouse-*Txnrd1*-R	GGGAGTGTCTTGGACGGGA
Mouse-*Txnrd2*-F	AAACCAGGACTTTGAATCTGGAG
Mouse-*Txnrd2*-R	GATGTGGGGAACAGAGGTAGC
Mouse-*Txnrd3*-F	GGCAACAGGGTGATGATCTTC
Mouse-*Txnrd3*-R	CTGGAAAGTTCGGTCACATCC
Mouse-*Txndc17*-F	AGGGCAAGACCATTTTCGC
Mouse-*Txndc17*-R	CCCTCTCGAATGACTGGCTC
Mouse-*Glrx1*-F	GCTCAGGAGTTTGTGAACTGC
Mouse-*Glrx1*-R	AGAAGACCTTGTTTGAAAGGCA
Mouse-*Glrx*2-F	ATCGTCGTTTTGGGGGAAGTC

Mouse-*Glrx*2-R	GGAACAGTAAGAGCAGGATGTTT
Mouse-*Glrx*3-F	CAGTGGTGGAAGTCGGCTC
Mouse-*Glrx*3-R	GCCATGACATCGTTCATCTGT
Mouse-*Nox1*F	GGTTGGGGCTGAACATTTTTC
Mouse-*Nox1*-R	TCGACACACAGGAATCAGGAT
Mouse-*Nox*2-F	TGTGGTTGGGGCTGAATGTC
Mouse-*Nox*2-R	CTGAGAAAGGAGAGCAGATTTCG
Mouse-*Gsr*-F	GACACCTCTTCCTTCGACTACC
Mouse-*Gsr*-R	CCCAGCTTGTGACTCTCCAC
Mouse-*Glut2*-F	TCAGAAGACAAGATCACCGGA
Mouse-*Glut2*-R	GCTGGTGTGACTGTAAGTGGG
Mouse-*Glut3*-F	ATGGGGACAACGAAGGTGAC
Mouse-*Glut3*-R	GTCTCAGGTGCATTGATGACTC
Mouse-*Glut4*-F	GTGACTGGAACACTGGTCCTA
Mouse-*Glut4*-R	CCAGCCACGTTGCATTGTAG
Mouse-*Hk1*-F	CGGAATGGGGAGCCTTTGG
Mouse-*Hk1*-R	GCCTTCCTTATCCGTTTCAATGG
Mouse-*Pfkl*-F	GGAGGCGAGAACATCAAGCC
Mouse-*Pfkl*-R	CGGCCTTCCCTCGTAGTGA
Mouse-*Pfkm*-F	TGTGGTCCGAGTTGGTATCTT
Mouse-*Pfkm*-R	GCACTTCCAATCACTGTGCC
Mouse-*Gapdh*-F	AGGTCGGTGTGAACGGATTTG
Mouse-*Gapdh*-R	TGTAGACCATGTAGTTGAGGTCA
Mouse-*Pkm2*-F	TGTGGTCCGAGTTGGTATCTT
Mouse-*Pkm2*-R	GCACTTCCAATCACTGTGCC

Mouse-*Ldha*-F	TGTCTCCAGCAAAGACTACTGT
Mouse-*Ldha*-R	GACTGTACTTGACAATGTTGGGA
Mouse-*Mdh1*-F	AGATTGCCTTCAAAGACCTGG
Mouse-*Mdh1*-R	GCAGTTCGTATTGGCTGGGT
Mouse-*Mdh2*-F	TTGGGCAACCCCTTTCACTC
Mouse-*Mdh2*-R	GCCTTTCACATTTGCTCTGGTC
Mouse-*Idh1*-F	ATGCAAGGAGATGAAATGACACG
Mouse-*Idh1*-R	GCATCACGATTCTCTATGCCTAA
Mouse-*Idh2*-F	GGAGAAGCCGGTAGTGGAGAT
Mouse-*Idh2*-R	GGTCTGGTCACGGTTTGGAA
Mouse-*Idh3a*-F	TGGGTGTCCAAGGTCTCTC
Mouse-*Idh3a*-R	CTCCCACTGAATAGGTGCTTTG
Mouse-*Idh3b*-F	TGGAGAGGTCTCGGAACATCT
Mouse-*Idh3b*-R	AGCCTTGAACACTTCCTTGAC
Mouse-*Idh3g*-F	GGTGCTGCAAAGGCAATGC
Mouse-*Idh3g*-R	TATGCCGCCCACCATACTTAG
Mouse-*Aco2*-F	ATCGAGCGGGGAAAGACATAC
Mouse-*Aco2*-R	TGATGGTACAGCCACCTTAGG
Mouse-*Atp5i*-F	GAGAAGGCACCGTCGATGG
Mouse-*Atp5i*-R	ACACTCTGAATAGCTGTAGGGAT
Mouse-*Atp5o*-F	TCTCGACAGGTTCGGAGCTT
Mouse-*Atp5o*-R	AGAGTACAGGGCGGTTGCATA
Mouse-*Cox6b1*-F	ACTACCTGGACTTCCACCG
Mouse-*Cox6b1*-R	ACCCATGACACGGGACAGA
Mouse-*Cox18*-F	GGCCGCCTATCAGCACTAC

Mouse-*Cox18*-R	TGAGATAAGTCTCCGCATGTTCT
Mouse-*Ndufb5*-F	CAAGAGACTGTTTGTCGTCAAGC
Mouse-*Ndufb5*-R	TGTTCACCAGTGTTATGCCAAT
Mouse-*G6pd*-F	CACAGTGGACGACATCCGAAA
Mouse-*G6pd*-R	AGCTACATAGGAATTACGGGCAA
Mouse-*Pgd*-F	TGAAGGGTCCTAAGGTGGTCC
Mouse-*Pgd*-R	CCGCCATAATTGAGGGTCCAG
Mouse-*Actin*-F	GGCTGTATTCCCCTCCATCG
Mouse-*Actin*-R	CCAGTTGGTAACAATGCCATGT

Luciferase primers	**Sequences**
Mouse-*Mllt3*-promoter-F	CCTGAGCTCGCTAGCCTCGAGGTGCAAACGC GGAATGGTCACC
Mouse-*Mllt3*-promoter-R	CAGTACCGGATTGCCAAGCTTCGAGCTAGCCA TGCCTGGGGG
Mouse-*Gata2*-promoter-F	CCTGAGCTCGCTAGCCTCGAGTCCCCCTCCCA CAGACATACAGAAA
Mouse-*Gata2*-promoter-R	CAGTACCGGATTGCCAAGCTTCGACTGCGGCG CGGTGGGC
Mouse-*Gata1*-promoter-F	CCTGAGCTCGCTAGCCTCGAGATAAAGCCTAA CTCTAACAGACCC
Mouse-*Gata1*-promoter-R	CAGTACCGGATTGCCAAGCTTCTTGGATATGG AGCTGGTAT
Mouse-*Pu.1*-promoter-F	CCTGAGCTCGCTAGCCTCGAGCTCTGATCAAA TGACTTGGCCCCA

Mouse-*Pu.1*-promoter-R	CAGTACCGGATTGCCAAGCTTAGGGGCGGTG AGGGAAAACC
Mllt3-F (for ChIP)	ACTCTTACAGACTTGGTTGGGAAAT
Mllt3-R (for ChIP)	TAACGGGAAGGAGGTTTCCTGGA
Gata2-F (for ChIP)	GACTATTAAAGATGGAAACAAATGCATG
Gata2-R (for ChIP)	GGGTTGAAGGTCACAGCACG
Gata1-F (for ChIP)	CCCCTCATGATGGCTCTTGGG
Gata1-R (for ChIP)	CCAAAGAGAAGGCAAAGACC
Pu.1-F (for ChIP)	CTCTGATCAAATGACTTGG
Pu.1-R (for ChIP)	AAAGACGTGGCCACCACAT
CUT&Tag primers	**Sequences**
Irf7-F (for q-PCR)	CTGAACCTAGGTGACCACAAGTTC
Irf7-R (for q-PCR)	CAGTCTGGGAGAATCAAAGTAGATG
Dhx58-F (for q-PCR)	CCCTACCAGTGGGAAGTGATCTTAC
Dhx58-R (for q-PCR)	AGCCATCTCCTGAACCAAGG